Charging and heating effects in a system of coupled single-electron tunneling devices

V. A. Krupenin,* S. V. Lotkhov, H. Scherer, Th. Weimann, A. B. Zorin, F.-J. Ahlers, J. Niemeyer, and H. Wolf
Physikalisch-Technische Bundesanstalt, Bundesallee 100, D-38116 Braunschweig, Germany
(Received 12 November 1998)

The effects of interaction in systems of capacitively coupled Al single-electron transistors were studied. Employing one device carrying a small current as an electrometer we observed the suppression of its modulation characteristic by applying a substantially greater current to the neighboring transistor. This is explained by the combined action of charge oscillations and dissipated power in the transistor island (both caused by intensive single-electron tunneling) on the electrometer island. We demonstrate that by changing the parameters and mutual location of the interacting transistors on an SiO_x substrate, the contribution of each effect can become dominant. [S0163-1829(99)07915-1]

INTRODUCTION

The single electron tunneling (SET) electrometer, i.e., a system of two series-connected junctions and a small island in between, supplied with a gate electrode,[1] is a sensitive device that allows charges to be measured in delicate experiments with single electrons (see, for example, Refs. 2 and 3). Since the coupling between the electrometer island and an island of an (SET) device under test is normally of the capacitive type, their close arrangement is common practice for accomplishing better coupling. In such a pair of coupled devices, the effects of their mutual interaction can, however, manifest themselves. For instance, the back influence of an electrometer was mentioned in the electron box experiment by Lafarge *et al.*[2] According to their evaluation, the intrinsic noise of an electrometer resulted in a noticeable increase in an effective temperature of the measured electron box. In a recent experiment with a multijunction SET trap,[4] the back action of an electrometer was even more prominent. Namely, the variation of the current supplied through the SET electrometer has influenced the storage performance of the SET trap in the sense that the dwelling times of the electrons stored in the memory island of the trap drastically decreased when the electrometer current was increased.

There are two main mechanisms of interaction in the system of coupled SET devices. Firstly, the heating of an island of a neighboring device via the substrate. Since a power dissipated inside a small island can be relatively large (up to 50% of the total power dissipated in a circuit[5]) and since the low-thermal conductivity of dielectric substrates hinders an efficient drain of heat from the island to the outside, this effect can be considerable. Secondly, the capacitive coupling can make the tunneling of single electrons in both devices interdependent so that, as result, their I-V curves are modified [see, for example, the experiment with coupled one-dimensional (1D) arrays by Delsing, Haviland, and Davidson[6]].

In this paper, we focus on the effect of the interaction between pairs of SET transistors. In contrast to Ref. 6, we investigate the regime when the bias currents are strongly unequal. Because of the low dissipation and the low frequency of SET events, the device biased by a lower current and functioning as a sensor (electrometer) is more susceptible to interaction. The modification of its I-V characteristics in the case of current variation in the coupled transistor is studied in this paper. Despite the fact that the effect of the SET oscillations and enhanced temperature on the electrometer I-V curve are almost similar (both ''round'' the Coulomb blockade region), we managed to distinguish them. Owing to deliberately different sizes of the junctions in pairs of interacting devices (resulting in a different relationship between SET effect strength and power dissipation) as well as a different distance between the islands, the data obtained provide a means for evaluating each effect separately.

CHARACTERISTICS OF THE SAMPLES

We have fabricated and measured two types of coupled transistors. Firstly, to ensure that the transistor pairs are well coupled and to exploit the same electrometer in combination with devices having different parameters, we have chosen a triple-transistor system with parallel arrangement of the islands positioned close together. Secondly, in order to minimize the heating effect, we positioned the islands of two transistors some distance apart and supplied them with an H-shaped metallic coupler in between, which enhanced their cross capacitance.

Our triple-transistor (sample 1) consists of three standard-type SET transistors with $Al/AlO_x/Al$ junctions prepared by the conventional shadow evaporation technique on a thermally oxidized (800 nm deep) Si substrate. The three-layer mask was made of polymethylmethacrylate (PMMA)/Ge/copolymer. After patterning the PMMA layer using e-beam exposure and a developing process, the pattern was transferred to the Ge layer by an etching process in a CF_4 plasma, followed by oxygen plasma etching of the copolymer layer. Due to the specific shape of the mask (similar to that used earlier for fabricating the twin-transistor system[7]) and the two-step evaporation of Al at appropriate angles, all three in-line shaped transistors were made without stray shadows of their islands [see micrograph in Fig. 1(a)]. The double transistor (sample 2) was made in a similar way by the double-angle evaporation technique. As a result of such evaporation, the H-shaped coupler also consisted of two Al layers [see Fig. 2(a)].

All transistors were galvanically isolated from one an-

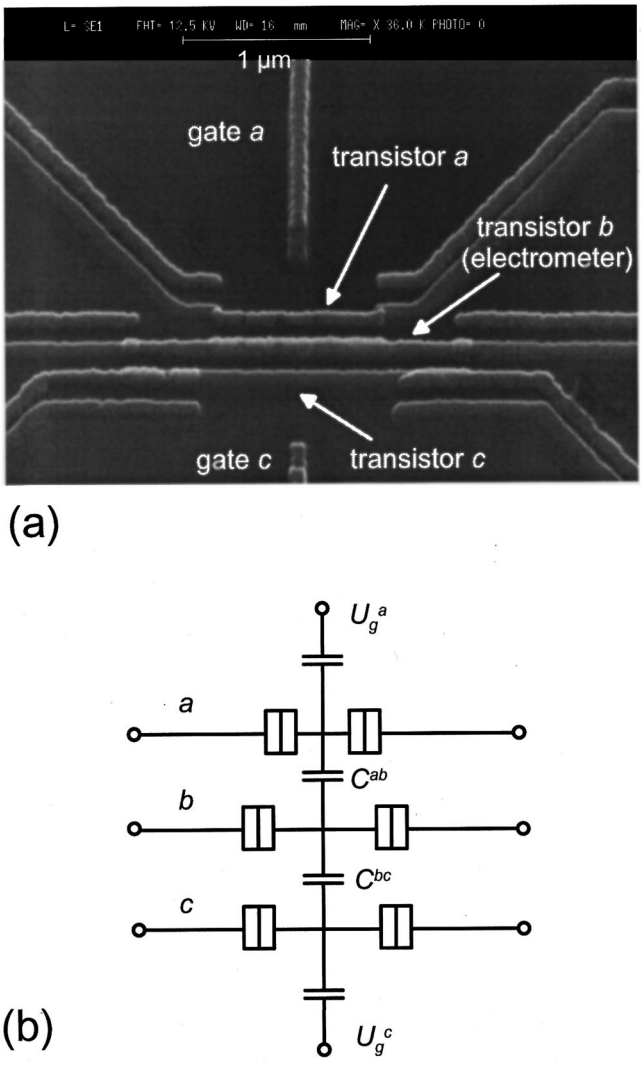

FIG. 1. (a) Scanning electron microscopy (SEM) photo of the triple-transistor device (sample 1). The structure was fabricated by the two-angle evaporation technique through a suspended mask, so that the island of transistor *b* consists of two layers. (b) The simplified equivalent electric circuit of this sample.

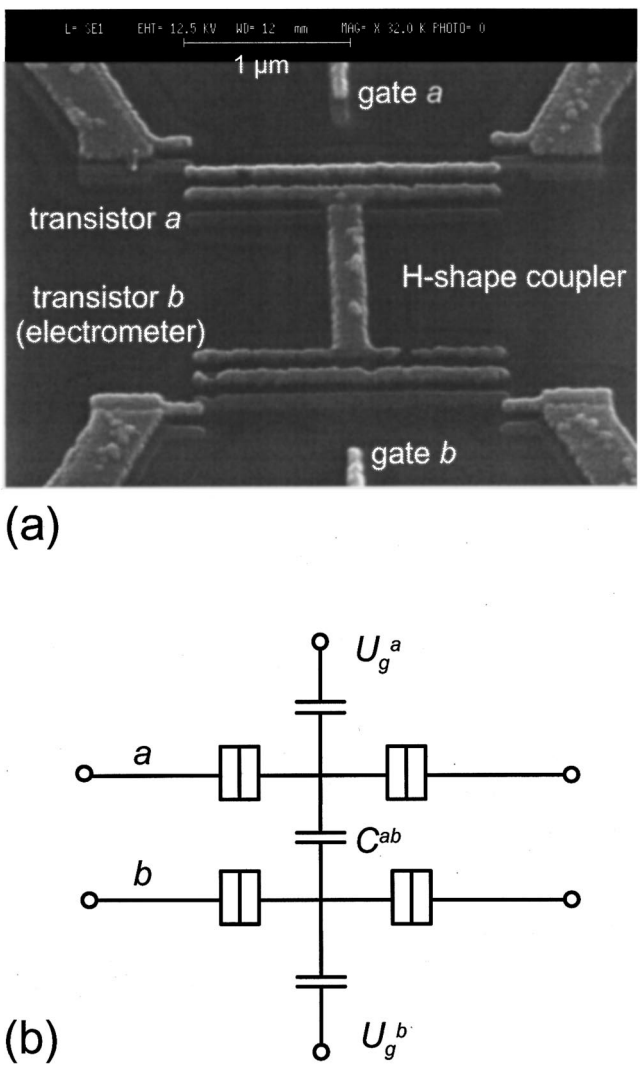

FIG. 2. (a) SEM photo of the *H* sample (sample 2). (b) The simplified equivalent electric circuit of this sample.

other so that independent biasing was possible (see equivalent circuit diagrams in Figs. 1(b) and 2(b)]. Two gate electrodes next to the two sides of the transistor structures were used to vary the offset charges on the transistor islands with a possibility of compensating the polarization on one of these islands by applying appropriate voltages to both gates.

In sample 1, the transistor parameters were intentionally varied within the array. Namely, the dimensions of the island of the smallest transistor *a* (topmost in Fig. 1) were about 75×900 nm, and the junction areas were about 40×50 nm, while the corresponding sizes of the largest transistor *c* (lowermost in Fig. 1) were about 75×1900 nm and 60×400 nm, respectively. The approximate distance between the centers of each two neighboring transistors was about 150 nm, so that the gaps separating the islands were about 75 nm only, which resulted in significant cross capacitances. The dimensions of the islands of sample 2 were about 100×1900 nm and their distance was about 1700 nm.

The electric parameters of each transistor were determined from the set of I-V, V-U_g, and I-U_g characteristics in a standard way (for details, see, e.g., Ref. 8). The coupling (cross) capacitances C^{ab} and C^{bc} were derived from measurements in a similar way as in the electron-box experiment.[2] The results are given in Tables I and II.

EXPERIMENT

The measurements were carried out in a top-loading dilution refrigerator within the temperature range from 25 to 75

TABLE I. The electric parameters of the triple-transistor sample (sample 1) obtained from measurements.

Triple-transistor parameters	Transistor *a* (small)	Transistor *b* (electrometer)	Transistor *c* (large)
C_Σ (aF)	320	620	2300
C_1/C_2	0.9	0.9	0.7
R_1+R_2 (MΩ)	2.0	1.16	0.275
R_1/R_2	1.2	1.5	1.6
C^{ab} and C^{bc} (aF)	32	50	

TABLE II. The electric parameters of the *H* sample (sample 2) obtained from measurements.

Double-transistor parameters	Transistor *a*	Transistor *b* (electrometer)
C_Σ (aF)	240	230
C_1/C_2	0.95	0.9
R_1+R_2 (MΩ)	5.8	5.3
R_1/R_2	~1	~1
C^{ab} (aF)	16	

mK. The aluminum transistors were driven to the normal state by application of a magnetic inductance *B* of 1 T. Commercial Thermocoax® cables about 1 m in length, serving as efficient microwave frequency filters,[9] were installed in the cold part of all electrical lines. The transistors were biased symmetrical with respect to ground using a voltage source and load resistors ($2\times 100\,\mathrm{M\Omega}$), that actually fixed the average current value and in fact met the conditions for electron tunneling which corresponds to the voltage bias case and low-environmental impedance (see, e.g., Ref. 10). We used this constant-current method to take advantage of the large voltage signal due to the large differential resistance $R_d = dV/dI$ at the low level of the electrometer current. The signal was amplified using a custom-made amplifier at room temperature and then read out by a commercial voltmeter.

As long as the most considerable variations of the electrometer *I-V* characteristic were expected in the Coulomb blockade region, we measured the V-U_g curves of the electrometers (denoted as *b* in both circuits) at low-bias current (1 pA in the triple transistor and 5 pA in the double transistor). For the triple-transistor sample, Figs. 3(a) and 4(a) show the effect of transport currents in transistors *a* and *c* on electrometer *b*, which implies that its gate modulation is gradually depressed. Two sets of currents $I^{(a)}$ and $I^{(c)}$ were chosen in such a way that they corresponded to the Joule losses, which are roughly equal in each device. One can see that at equal powers, the current $I^{(a)}$ causes a markedly larger depression of the modulation than $I^{(c)}$ does.

In so far as the characteristic charging energies ($e^2/2C$) of transistors *a* and *c* in sample 1 were intentionally made unequal, $E_C^a/k_B \sim 2.9\,\mathrm{K}$ and $E_C^c/k_B \sim 0.4\,\mathrm{K}$, we can expect that the difference in the sets of curves presented in Figs. 3(a) and 4(a) is due to the very different effect of single-electron tunneling in each transistor. However, since this difference was not very large, we arrived at the conclusion that the heating effect in the system was substantial. This is why we have carried out simulations of the coupled transistors taking into account the enhanced temperatures of their islands.

The charging energies of both transistors of sample 2 were rather high (~4 K) and this led, in particular, to the electrometer characteristic becoming less sensitive to a finite increase in the temperature of its island. Moreover, the design of this sample with the larger distance between the transistors substantially impeded the heating of the electrometer island. Figure 5(a) demonstrates the influence of the transport current in transistor *a* on electrometer *b*. As we will show below, this effect is attributed to mostly SET oscillations in the coupled transistor.

MODELING

In the framework of the orthodox theory,[11] the dynamics of the multijunction SET system is generally described by the master equation for the total probability density σ_{tot}, which in the case of two interacting transistors (say, *a* and *b*) depends on two variables, n^a and n^b, the populations of their islands. Our case is characterized by a small coupling coefficient λ, determined as the dimensionless charge $\Delta Q_0/e$ induced on the electrometer island due to charging of the transistor island by a charge *e*. In terms of the equivalent circuits [Figs. 1(b) and 2(b)].

$$\lambda = \Delta Q_0/e \approx C^{ab}/C_\Sigma^{(a)} \ll 1. \tag{1}$$

In addition, we consider strongly dissimilar regimes,

$$I^{(a)} \gg I^{(b)}. \tag{2}$$

The assumptions Eqs. (1) and (2) make it possible to drastically simplify the modelling of the coupled transistors by neglecting the back influence of the electrometer *b* on the active transistor *a*. Owing to the low current $I^{(b)}$, the rate of SET events in the electrometer, $\sim 2I^{(b)}/e$, is rather small and the jumps of its island's potential are moderate, $\sim e/C_\Sigma^{(b)}$ (i.e., the electrometer is almost switching between the states $n^{(b)}=0$ and $n^{(b)}=1$). Therefore the neighboring device, operating at much higher current, experiences these rare and, due to Eq. (1), small variations of its offset charge. These variations do not considerably change its operation regime nor the stationary distribution function of the charge states of its island, $\sigma^{(a)}(n)$.

On the contrary, the variations of the offset charge Q_0 on the electrometer's island due to intensive SET in the coupled device are substantial,

$$Q_0(t) = Q_{00} + \lambda n^{(a)}(t) e, \tag{3}$$

where Q_{00} is the offset charge of a decoupled electrometer and $n^{(a)}$ the instant number of excess electrons on the transistor island. As long as the energy corresponding to the rate of current [$\sim(2\pi\hbar)I^{(a)}/e \leqslant 5\ \mu\mathrm{eV}$] is considerably smaller than characteristic charging energies, the variations $n^{(a)}(t)$ can be considered slow. Then the electrometer dynamics can be found from solving a master equation for $\sigma^{(b)}(n)$ with time-dependent parameters, namely the rates $\Gamma_j^{\pm}[Q_0(t)]$ of SET in each junction $j=1,2$ and in both directions $\pm$. Solving that equation is drastically simplified within the limit of Eq. (2) allowing to replace $\Gamma_j^{\pm}$ by their average values,

$$\overline{\Gamma_j^{\pm}} = \tau^{-1} \int_{\text{over}\,\tau} \Gamma_j^{\pm}[Q_0(t')]\,dt'$$

$$= \sum_{n^a} \sigma^{(a)}(n^{(a)}) \Gamma_j^{\pm}[Q_0(n^{(a)})], \tag{4}$$

where τ is the time interval which much exceeds $e/I^{(a)}$. Note that this procedure does not modify the original rates (except a shift in argument Q_0) if they behave linearly with Q_0. This corresponds to the case when the electrometer is biased well above the blockade voltage so that the variations of Q_0 fall within the linear rise of $\Gamma_j^{\pm}$. However, when the electrometer is biased by very low current, it operates in the regime of

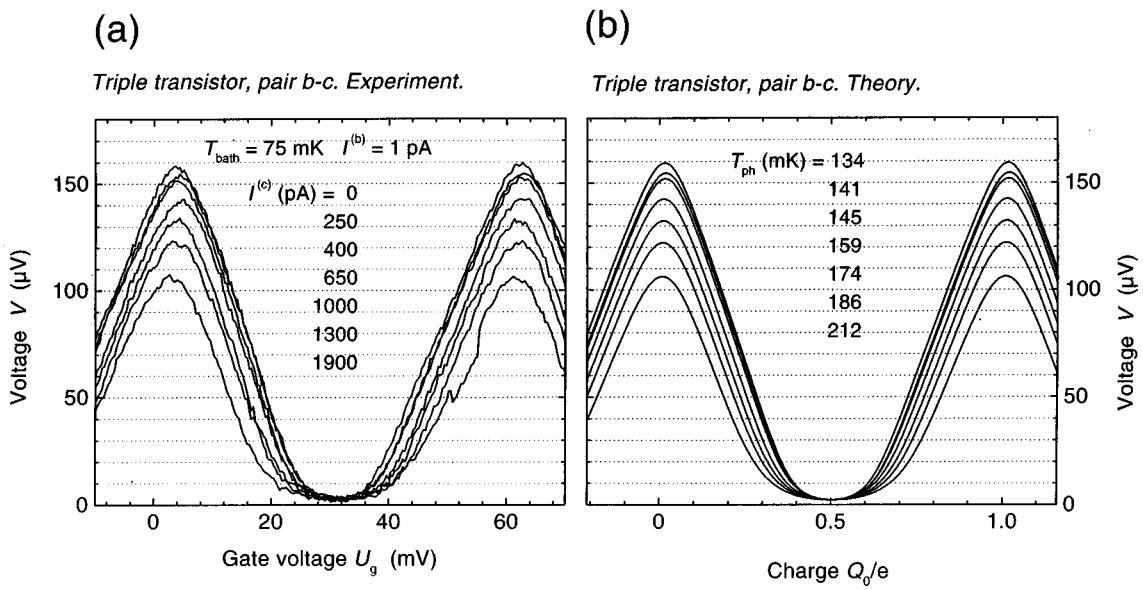

FIG. 3. (a) Experimental modulation curves of electrometer *b* in sample 1 measured at several current values in (large) transistor *c*. The effect of SET oscillations was found to be small in this case. (b) The theoretical curves were plotted with the electron temperature of the electrometer island as a fitting parameter.

nonlinear dependence $\Gamma_j^{\pm}(Q_0)$ and, therefore, the averaging Eq. (4) leads to nonvanishing corrections to the rates: the broader the distribution $\sigma^{(a)}(n^{(a)})$, the larger these corrections. This is the principle of our rectification of SET oscillations.

Other modifications of the simulation scheme concern a careful consideration of the electron temperature T_e of the electrometer island and of cotunneling. In a realistic case of very dissimilar electron temperatures of an island and the leads, the expression for the tunneling rates takes the form

$$\Gamma_j^{\pm}(n)=k_BT_e/(e^2R_j^{(b)})\ln\{1+\exp[E_j^{\pm}(n)/k_BT_e]\}, \quad (5)$$

where T_e is assumed to be higher than twice that of the counter electrodes.[5] That is why the latter drops out of expression Eq. (5). Finally, the cotunneling current component[12] was also taken into account.

FITTING PROCEDURE

1. Sample 1 (triple transistor sample)

As the electrometer almost operated in the Coulomb blockade regime, in which it was extremely sensitive not only to charge but also to temperature, particular emphasis has been laid on the determination of all relevant tempera-

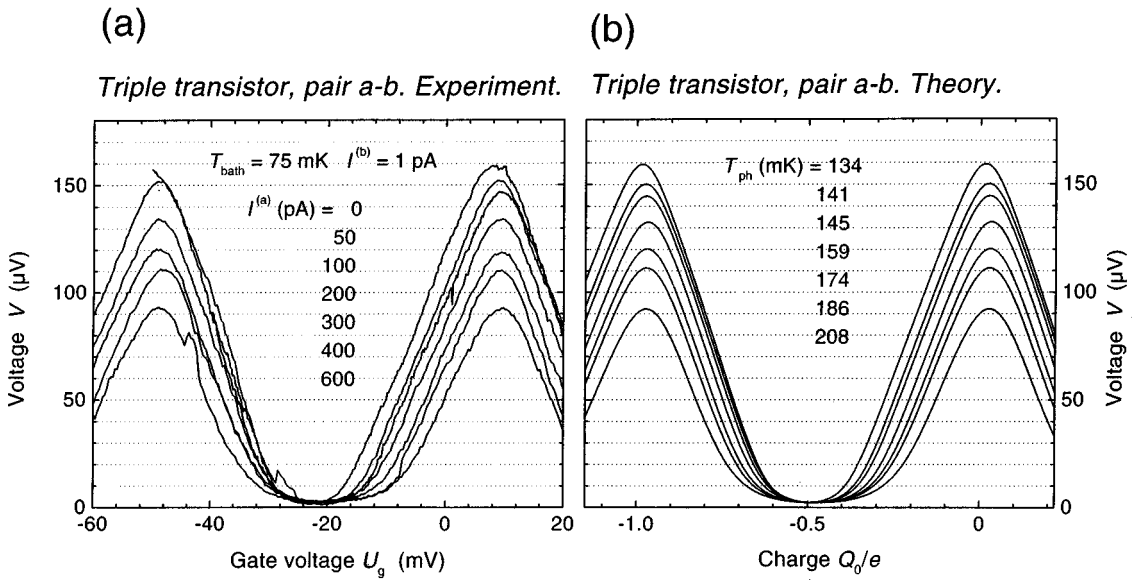

FIG. 4. (a) Experimental modulation curves of electrometer *b* in sample 1 measured at several current values in (small) transistor *a*. The effect of shot noise was found to be considerable in this case. (b) The theoretical curves were plotted without fitting parameters but using the plot T^b vs the total power (Fig. 6).

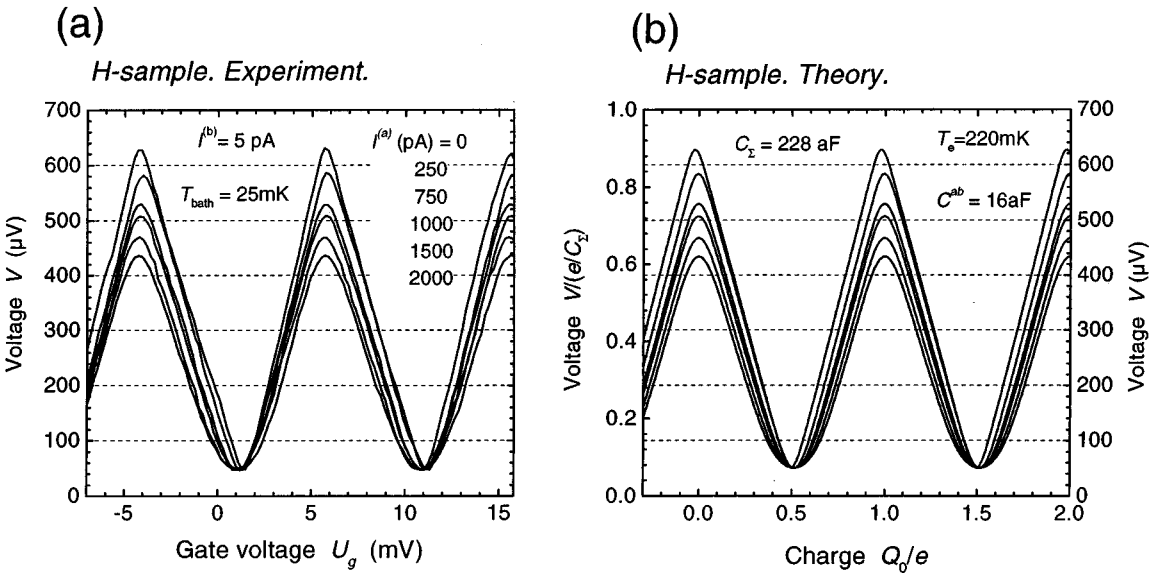

FIG. 5. (a) Experimental modulation curves of electrometer *b* in sample 2 measured at several current values in transistor *a*. The effect of heating was found to be negligibly small in this case. (b) The theoretical curves were plotted using C^{ab} as a fitting parameter.

tures. First, we assumed that the on-chip leads ensured good thermal contact between the bath and the outer electrodes of the electrometer junctions. The heat drain was realized through the double-layer Al films that were $25+35\,\mathrm{nm}=60\,\mathrm{nm}$ thick, 20-μm wide and a few-mm long and connected to much larger contact pads. Evaluating the thermal conductivity of the normal-state Al at 75 mK using the Wiedemann-Franz law as $\kappa_{\mathrm{Al}}\sim 10^{-2}-10^{-3}\,\mathrm{W/K/m}$, we estimated the thermal conductance of these films to be about $10^{-10}-10^{-11}\,\mathrm{W/K}$. For the maximum dissipated power in the electrometer of about $1.5\times 10^{-16}\,\mathrm{W}$, it resulted in a negligibly small increase in temperature (<0.02 mK) in the counter electrodes. Thus, we assumed that their phonon and electron temperatures were maintained equal to the bath temperature $T_{\mathrm{bath}}=75\,\mathrm{mK}$. On the contrary, the electron temperature T_e in the electrometer island substantially exceeded this temperature because of poor electron-phonon coupling at low temperatures (see, for instance, Refs. 5 and 13). Such an effect can be described by the model by Roukes *et al.*[14] according to which $T_e=(T_{\mathrm{ph}}^5+P/\Sigma\Omega)^{1/5}$, where T_{ph} is the phonon temperature of the island, P the power dissipated in the island of volume $\Omega\approx 7\times 10^{-3}\,\mu\mathrm{m}^3$, and $\Sigma_{\mathrm{Al}}\approx 0.2-0.6\,\mathrm{nW/K^5/\mu m^3}$ (Refs. 5 and 13) the material constant. Since any reasonable (although small) value of thermal conductivity of the SiO_2 substrate, $\kappa_{\mathrm{SiO2}}\sim 10^{-4}\,\mathrm{W/K/m}$ at $T\sim 0.1\,\mathrm{K}$ (see the data for vitreous silica in Ref. 15), provides a negligibly small increase in temperature $\Delta T_{\mathrm{ph}}\sim P/(S^{1/2}\kappa_{\mathrm{SiO2}})<10^{-5}\,\mathrm{K}$ for the contact area S of about $10^{-13}\,\mathrm{m}^2$ and power $P\sim 10^{-16}\,\mathrm{W}$, we concluded that $T_{\mathrm{ph}}=T_{\mathrm{bath}}$ when the neighboring transistors were off. The best fitting curve corresponds to $T_e\approx 134\,\mathrm{mK}$ in the regions of tops of the modulation curve measured for $I=1\,\mathrm{pA}$. This number allows the value of $\Sigma_{\mathrm{Al}}\approx 0.23\,\mathrm{nW/K^5/\mu m^3}$ to be restored, although the accuracy of such a reconstruction procedure is poor, since this value is largely sensitive to T_e. We therefore restrict ourselves to the conclusion that the value of Σ_{Al}, obtained as a by product, is within the range furnished by literature.[5,13]

Next, we fitted the electron temperature for the electrometer modulation curves taken when transistor *c* operated, i.e., the device which, as the simulations have shown, produced almost heat (see Fig. 2). As the power dissipated in the neighboring transistor increased, T_{ph} (as well as T_e) increased as well. The phonon temperature in the leads remained equal to T_{bath} because of the large (mm scale) length $l_{e\text{-ph}}$ of the electron-phonon interaction. The dependencies of T_e and T_{ph} versus the total power dissipated in transistor *c* are shown in Fig. 6.

To account for the heating effect in the case of the transistor pair *a*-*b* (Fig. 3), where it occurs together with the

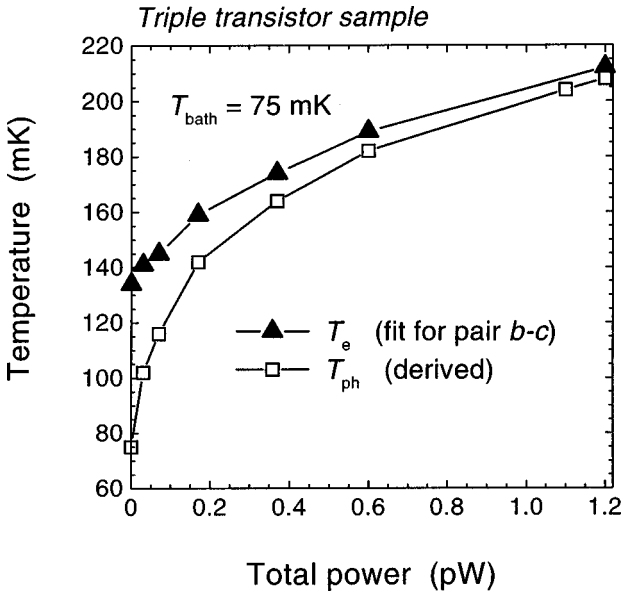

FIG. 6. Electron temperature T^b of the electrometer island as a function of the total power dissipated in the neighboring transistor *c* (upper curve). The phonon temperature of the electrometer island is derived from the model by Roukes *et al.*[14] with $\Sigma_{\mathrm{Al}}=0.23\,\mathrm{nW/K^5/\mu m^3}$.

effect of large fluctuations of the polarization charge, we supposed that the heating was identical to that for pair b-c. Although the widths of islands a and c as well as the distances from the electrometer island were identical, the island of transistor a, as seen in Fig. 1(a), was approximately twice shorter. On the other hand, as long as the phonon wavelengths at low temperature ($\lambda_{ph} \sim \hbar \nu_{sound}/k_B T \sim 0.3\,\mu$m at 0.1 K) were larger than the thicknesses of Al layers and comparable with the in-plane dimensions of the islands, the temperature gradients were small on this scale. Hence, we concluded that in both cases the temperature T_{ph} was distributed almost uniformly over the length of the electrometer island and it was determined only by the power dissipated in a side transistor.

On the basis of this assumption, we computed the series of curves for those electron and phonon temperatures that correspond to the same power dissipated in the case of pair b-c. As a result, the curves obtained without additional fitting parameters were found to be in good agreement with the experiment [see Fig. 3(b)].

2. Sample 2 (H sample)

First, using the Roukes model we evaluated the electron temperature of the electrometer island at bias current $I^{(b)} = 5$ pA and zero current in transistor a. We got $T_e \approx 220$ mK ($\gg T_{bath} \approx 25$ mK), and by fitting capacitance $C_\Sigma^{(b)}$ we arrived at the value of 228 aF [compare the pair of the topmost curves in Figs. 5(a) and 5(b)]. Note that this value of capacitance is nearly the same as that obtained from the I-V curve measurements ($\approx$230 aF). Then, the curves corresponding to the case $I^{(a)} \neq 0$ were computed on the assumption of constant temperature $T_e = 220$ mK. They were fitted with the only parameter C^{ab}, and the best fit curves gave the value of 16 aF, that is in fact the value found in the electron-box measurements (see Table II).

In order to rule out the heating effect, we roughly evaluated[13] the enhancement ΔT_s of the temperature of the substrate under the electrometer island that was caused by power dissipation in transistor a. Assuming a spherical geometry and the aforementioned value of κ_{SiO2},[15] we found $\Delta T_s \sim 100$ mK for the case of maximum dissipation $P = 20$ pW corresponding to $I^{(a)} = 2$ nA. Such a value of ΔT_s has practically no effect on T_e and, therefore, on the modulation amplitude. Hence, these measurements unambiguously demonstrate the effect of rectification the SET oscillations.

Owing to very large resistances of the tunnel junctions, the electrometer behavior was well described by the orthodox model. One can see in Fig. 5(a) that the shape of the modulation curve corresponding to zero current in transistor a is very close to a triangular one. In modelling this sample we did not make the cotunneling corrections, what made the fitting procedure more reliable. As can be seen in Fig. 5, the experimental and theoretical curves are in very good agreement.

DISCUSSION

We have shown that in the system of SET transistors positioned close to one another, the interaction of the devices proceeds through a transfer of heat and gating of a device by fluctuations of the island potentials. These effects can be most clearly seen in modulation curves of the other device measured at low-bias currents corresponding to the Coulomb blockade nonlinearity in the I-V curve.

The results obtained show that in the case of the standard substrate (several hundred nm SiO_2 on the top of the Si plate) and low temperature ($<$100 mK) a local overheating of the substrate can be considerable even at moderate power values (pW). As a result, the island of a transistor positioned nearby ($\sim$100 nm in the triple-transistor sample) is heated and the increase in its effective electron temperature can be observed in the modulation curves. On the other hand, a pair of more distant islands ($\sim$1.7 μm in the H sample) is substantially less subjected to this effect.

Moreover, due to capacitive coupling, the SET oscillations of the island potential in the transistor carrying a finite current cause fast variations of the polarization charge on the electrometer island. Since the working transistor was effectively voltage biased, these SET oscillations were incoherent[16] and characterized by am almost flat spectrum with the cutoff frequency $\omega_c \sim I/e$.[17] This broadband signal was perceived by the electrometer as a background charge noise. As long as the power density of this noise within the electrometer's bandwidth was too small for a straightforward measurement, we succeeded in detecting the noise by exploiting the nonlinear characteristic of the electrometer. In the framework of the orthodox theory of SET, we suggested the simple model for two coupled transistors in the regime of very dissimilar current. The simulations showed that the rectification of the SET oscillations can be well described by this model. Thus, we demonstrated the capability of an SET electrometer to develop a noise signal whose bandwidth considerably exceeds the electrometer's output bandwidth.

ACKNOWLEDGMENTS

This work was supported by the EU (MEL ARI Research Project No. 22953 CHARGE), the German BMBF (Grant No. 13N6260), the Russian Fund for Fundamental Research (Project No. 95-02-04151A), and the Russian Scientific Programm ''Physics of Solid-State Nanostructures.''

*Permanent address: Laboratory of Cryoelectronics, Department of Physics, Moscow State University, 119899 Moscow, Russian Federation.

[1] T. A. Fulton and G. J. Dolan, Phys. Rev. Lett. **59**, 109 (1987).

[2] P. Lafarge, H. Pothier, E. R. Williams, D. Esteve, C. Urbina, and M. H. Devoret, Z. Phys. B **85**, 327 (1991).

[3] M. W. Keller, J. M. Martinis, N. M. Zimmermann, and A. H. Steinbach, Appl. Phys. Lett. **69**, 1804 (1996).

[4] V. A. Krupenin, S. V. Lotkhov, D. E. Presnov, A. B. Zorin, F. J. Ahlers, J. Niemeyer, H. Scherer, Th. Weimann, and H. Wolf, Czech. J. Phys. **46-S4**, 2283 (1996); V. A. Krupenin, S. V. Lotkhov, and D. E. Presnov, Zh. Eksp. Teor. Fiz. **111**, 344 (1997) [JETP **84**, 190 (1997)].

[5] R. L. Kautz, G. Zimmerli, and J. M. Martinis, J. Appl. Phys. **73**, 2386 (1993).

[6] P. Delsing, D. B. Haviland, and P. Davidson, Czech. J. Phys. **46-S4**, 2359 (1996).

[7] A. B. Zorin, F. J. Ahlers, J. Niemeyer, Th. Weimann, H. Wolf, V.

A. Krupenin, and S. V. Lotkhov, Phys. Rev. B **53**, 13 682 (1996).
[8] T. M. Eiles, G. Zimmerli, H. D. Jensen, and J. M. Martinis, Phys. Rev. Lett. **69**, 148 (1992).
[9] A. B. Zorin, Rev. Sci. Instrum. **66**, 4296 (1995).
[10] G. L. Ingold and Yu. V. Nazarov, in *Single Charge Tunneling*, Vol. 294 of *NATO Advanced Studies Institute, Series B: Physics*, edited by H. Grabert and M. H. Devoret (Plenum, New York, 1992), p. 21.
[11] D. V. Averin and K. K. Likharev, in *Mesoscopic Phenomena in Solids*, edited by B. L. Altshuler, P. A. Lee, and R. A. Webb (North-Holland, Amsterdam, 1991), p. 176.
[12] D. V. Averin and Yu. V. Nazarov, Phys. Rev. Lett. **65**, 2446 (1990).
[13] J. P. Kauppinen and J. P. Pekola, Phys. Rev. B **54**, R8353 (1996).
[14] M. L. Roukes, M. R. Freeman, R. S. Germain, R. C. Richardson, and M. B. Ketchen, Phys. Rev. Lett. **55**, 422 (1985).
[15] R. C. Zeller and R. O. Pohl, Phys. Rev. B **4**, 2029 (1971).
[16] K. K. Likharev, IBM J. Res. Dev. **32**, 144 (1988).
[17] A. N. Korotkov, Europhys. Lett. **43**, 343 (1998).